

## Harmonic Emission from the Rear Side of Thin Overdense Foils Irradiated with Intense Ultrashort Laser Pulses

U. Teubner,<sup>1,2</sup> K. Eidmann,<sup>1</sup> U. Wagner,<sup>3</sup> U. Andiel,<sup>1</sup> F. Pisani,<sup>1</sup> G. D. Tsakiris,<sup>1</sup> K. Witte,<sup>1</sup> J. Meyer-ter-Vehn,<sup>1</sup> T. Schlegel,<sup>4</sup> and E. Förster<sup>3</sup>

<sup>1</sup>Max-Planck-Institut für Quantenoptik, D-85748 Garching, Germany

<sup>2</sup>Institut für Mikrotechnik Mainz GmbH, D-55129 Mainz, Germany

<sup>3</sup>Institut für Optik und Quantenelektronik, Friedrich-Schiller Universität, D-07743 Jena, Germany

<sup>4</sup>Gesellschaft für Schwerionenforschung mbH, D-64291 Darmstadt, Germany

(Received 25 November 2003; published 4 May 2004)

The harmonic emission from thin solid carbon and aluminum foils, irradiated by 150 fs long frequency-doubled Ti:sapphire laser pulses at  $\lambda = 395$  nm and peak intensities of a few  $10^{18}$  W/cm<sup>2</sup>, has been studied. In addition to the harmonics emitted from the front side in the specular direction, we observe harmonics up to the 10th order, including the fundamental from the rear side in the direction of the incident beam, while the foil is still strongly overdense. The experimental observations are well reproduced by particle-in-cell simulations. They reveal that strong coupling between the laser-irradiated side and the rear side occurs via the nonlocal electron current driven by the laser light.

DOI: 10.1103/PhysRevLett.92.185001

PACS numbers: 52.38.-r, 42.65.Ky, 52.25.Os

Current subpicosecond laser systems allow the study of laser-plasma interaction in a new regime of large values of  $I\lambda_0^2$  up to  $\approx 10^{20}$  (W/cm<sup>2</sup>) $\mu\text{m}^2$ , where  $I$  is the laser intensity and  $\lambda_0$  the wavelength [1]. One of the new processes occurring at these intensities is the generation of high harmonics from solid targets. After their observation in the early 80's with intense CO<sub>2</sub> laser pulses in the nanosecond regime [2], harmonic generation in the extreme ultraviolet has been demonstrated in many experiments with ultrashort pulse lasers [3–9] with the record up to the 75th order of the fundamental [5]. In parallel, numerous theoretical studies have been performed, mainly on the basis of particle-in-cell (PIC) simulations [10,11]. Besides the fact that high harmonics from solid targets have the potential for bright coherent ultraviolet light sources, including the possibility to generate atto-second pulses [12], they also contribute to improve the understanding of the complex laser-plasma interaction at high intensities [7,13].

Harmonics have been mainly observed in reflection from the front side of massive solid targets. Here we report for the first time harmonic emission from the rear side of thin foils with thicknesses of a fraction of  $\lambda_0 = 395$  nm in a “modest” intensity range below the relativistic limit  $a_0 = 1$ , with  $a_0^2 = I\lambda_0^2/1.37 \times 10^{18}$  (W/cm<sup>2</sup>) $\mu\text{m}^2$  the normalized field amplitude. We have checked that for our conditions the foils remain strongly overdense during the interaction time. Since the overdense plasma is opaque for frequencies below its plasma frequency  $\omega_p$ , one would expect that only harmonics above  $\omega_p$  are transmitted from the front to the rear. This effect may occur at very high intensities  $a_0 > 1$  [6,14]. However, for our conditions we observe, in agreement with our PIC calculations, strong rear side emission of the harmonics below  $\omega_p$ , including the fundamental at

the frequency  $\omega_0 = 2\pi c/\lambda_0$ , while at  $\omega_p$  a strong cutoff occurs. We note that the observations reported here are different from other phenomena such as anomalous transparency [15] or hole burning [16], which occur at extremely high intensities in the relativistic regime.

The experimental setup is schematically shown in Fig. 1(a). We have used frequency-doubled pulses from a 10 Hz Ti:sapphire laser system emitting 150 fs laser pulses of 230 mJ energy at a wavelength of 790 nm. To avoid early expansion of the thin foils by preplasma formation and to assure a steep density gradient

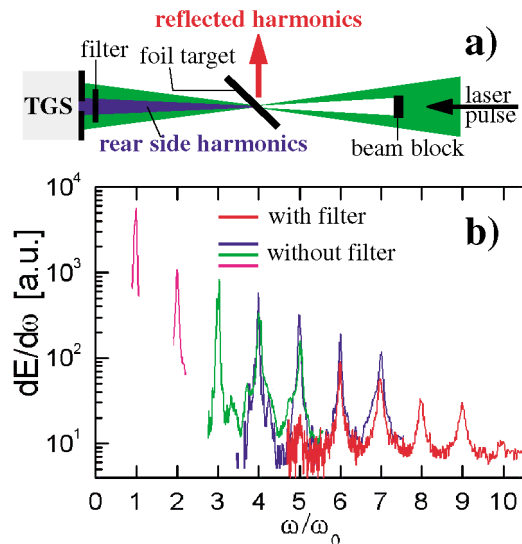


FIG. 1 (color). (a) Scheme of the experimental setup (see text). (b) Typical harmonic spectra measured at the rear side of a 60 nm carbon foil in different spectral windows, either with filter (no beamblock) or without filter (with beamblock). The fundamental and 2nd harmonic spectra were obtained from the diffraction at the support grating.

necessary for efficient harmonic generation [7], the laser light was frequency doubled to  $\lambda_0 = 395$  nm. From the measurement of the prepulse intensity performed at 790 nm, we expect at  $\lambda_0 = 395$  nm a contrast ratio  $\leq 1:10^{10}$  at  $t > 2$  ns and  $\leq 1:10^8$  at  $2$  ns  $> t > 1$  ps, where  $t$  is the time before the pulse maximum. After a set of four multilayer mirrors that reduce the remaining unconverted laser light by a factor of  $> 10^7$ , the blue light was focused by a  $f/2.5$  off-axis multilayer-coated parabolic mirror to a focal spot of  $5 \mu\text{m}$  diameter containing 50% of the energy. This yields an average intensity of  $1.5 \times 10^{18}$  W/cm<sup>2</sup>, while the peak intensity at the center was  $\approx 5 \times 10^{18}$  W/cm<sup>2</sup>.

The laser pulses were incident  $p$  polarized under an angle  $\alpha = 45^\circ$  on thin foils of aluminum or carbon 50 up to 400 nm thick. The emitted harmonic spectra from single shots were recorded by a transmission grating spectrograph (TGS) described in detail in [9]. The transmission grating (TG) had 1000 lines per mm, which were fixed on a perpendicular support grid with  $33 \mu\text{m}$  width. A 100 nm thick aluminum filter was mounted in front of the TGS to avoid damage by the fundamental laser light. In some shots this filter was removed to detect the low order harmonics emitted from the rear side of the foil. To also avoid damage of the diagnostics in this case, a small beam stop was placed between the focusing parabola and the target. It was adjusted in such a way that without the target no light could enter the spectrometer. As a consequence of the Al filter transmission, the spectral window of the TGS was in the range of 17 to 82 nm (the spectral window accessible in a single shot was limited by the size of the detector, but could be changed by moving the detector). Without the Al filter, the spectral range was extended to 150 nm (limited by mechanical constrains in positioning the detector). Data for the fundamental and the 2nd harmonic were obtained by analyzing the diffraction pattern of the support grid. Examples of spectra recorded in the different spectral windows are displayed in Fig. 1(b). In addition to the harmonics emitted from the rear side of the foil, we also studied reflected harmonics, but only with the 100 nm Al filter, i.e., harmonic orders  $\geq 5$ .

By integrating the harmonic lines over frequency, the conversion efficiency of laser light into harmonics was obtained. It is plotted in Fig. 2(a) for the case of a 60 nm thick carbon foil. The values for the 3rd to the 10th harmonic are obtained from the TG spectra. The efficiency of the 1st and 2nd harmonic, with respect to that of the higher harmonics, was estimated from the relative diffraction efficiencies of the TG (in the first order) and the support grating (at various diffraction orders). The error bars are mainly due to shot to shot fluctuations of the harmonic spectra; the accuracy of the individual single shot spectra was higher. An absolute value was obtained by fitting the relative spectrum of the TGS to the result of an independent measurement with a calibrated photo diode, which measured absolutely the fun-

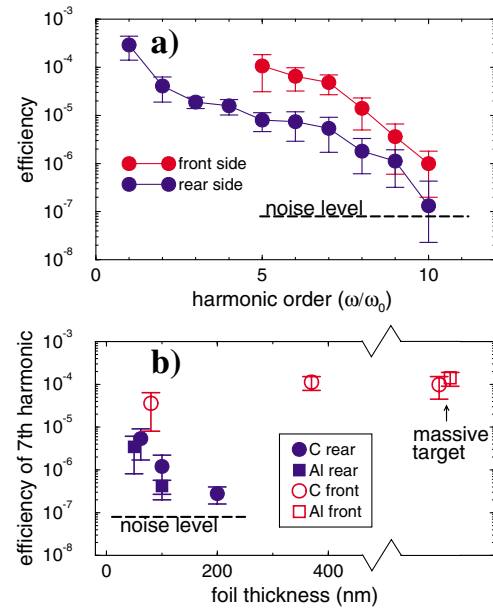


FIG. 2 (color). (a) Efficiencies of harmonics emitted from the rear and front side of a 62 nm thick carbon foil. (b) Efficiency of the 7th harmonic as a function of foil thickness for rear and front side observation for Al and C. For comparison, the efficiency obtained from a massive target [9] is displayed as well.

damental and 2nd harmonic emitted from the rear side into the full solid angle [17].

The measured efficiencies of the rear side harmonics decrease rapidly from the 1st to the 3rd followed by a slower decrease up to the 7th harmonic. Then the efficiency drops stronger, in particular, from the 9th to the 10th harmonic by a factor of  $\approx 10$ . Above this cutoff, no rear side harmonics exceeding the experimental noise limit could be identified. For comparison, we also plotted the efficiencies of the reflected harmonics, which, albeit more intense, exhibit a similar dependence on the harmonic order as the rear side harmonics.

A series of measurements was made for foils of different thickness. Figure 2(b) shows the results of the 7th harmonic emitted to the rear and the front side from C and Al targets. The rear side emission decreases strongly, with foil thickness approaching the experimental noise level for 200 nm. The emission from the front side is larger than the rear side emission even for the thinnest of the foils. It increases with increasing foil thickness and reaches the value for massive targets at 400 nm. It is also seen that within the shot to shot fluctuations no difference between the two target materials C and Al is apparent.

Variation of the laser intensity  $I_L$  revealed that high harmonics at the rear side were still present when we reduced the intensity by a factor of 10. Their efficiency scales in a similar way as was observed for front side harmonics from massive targets [9]. For example, the efficiency of the 7th harmonic changes as  $\eta_7 \propto I_L^\alpha$ , with  $\alpha$  between 1 and 2.

We will now discuss our experimental findings. To ascertain that the thin foil remains overdense during the interaction with the laser pulse, we have performed hydrodynamic calculations with the MULTI-FS code [18], using as input the temporal shape of the laser pulse corresponding to our experimental conditions, i.e., including the weak pedestal. At the time when the main pulse starts ( $\approx 150$  fs before the peak), the density gradient length is small ( $\approx 0.1\lambda_0$ ), and, midway between front and rear side, the foil is still at solid density. At such high densities, the transparency of the foil ( $e^{-d_f/d_s}$ , with  $d_f$  and  $d_s$  the foil thickness and skin depth, respectively) is very small for the harmonics below  $\omega_p$ , which is for a fully ionized Al or C foil of solid density close to the 9th harmonic (e.g., for the first harmonics of the order  $q \leq 3$ , the transparency is  $< 10^{-7}$ , which is below our noise level). As indicated by our hydrocode calculations as well as by our PIC simulations presented below, the foil expands only slightly during the interaction with the main pulse because of its inertia and the short pulse duration. Furthermore, since one-dimensional expansion is a reasonable assumption (foil thickness is small compared to spot diameter), the areal mass is conserved and the transparency even decreases with expansion, as long as the foil does not become underdense. This is because  $d_s \propto c/\omega_p \propto 1/\sqrt{n_e}$  while  $d_f \propto 1/n_e$ . Thus, we cannot interpret the observed rear side harmonic spectra as due to harmonics generated at the front side and transmitted through the foil to the rear side.

To investigate the role of the kinetic effects expected at the high intensities of the experiment, we have performed PIC calculations with the one-dimensional LPIC code [10]. It allows one to treat oblique incidence by a transformation into a moving frame. We have chosen input parameters close to the experimental conditions noted in the following as standard parameters:  $a_0 = 0.5$  (corresponding to an intensity  $2 \times 10^{18}$  W/cm<sup>2</sup>), angle of incidence =  $45^\circ$  at  $p$  polarization, pulse duration = 100 periods (at  $\lambda_0 = 400$  nm one period is 1.33 fs long), foil thickness =  $0.2\lambda_0$ , and  $n_e/n_c = 84$  (corresponding to 10 times ionized Al or nearly fully ionized C at solid density). The size of the simulation box was  $15\lambda_0$ . The ions are assumed to be mobile, and an initially sharp boundary between the foil and vacuum has been used.

The simulated spectrum for the standard parameters is shown in Fig. 3. As seen, the LPIC simulations reproduce the main features of the experiment. Intense rear side harmonic emission is observed at low harmonic orders, including the fundamental. Furthermore, around the 9th harmonic, a sharp cutoff is seen and higher harmonics have low intensities close to the numerical noise limit. Of interest is that the cutoff position coincides with the plasma frequency of the dense foil:  $\omega_p/\omega_0 = \sqrt{84} \approx 9.2$ . In fact, when we change the initial density, we observe a shift of the cutoff. The green curve in Fig. 3 shows a transmitted spectrum for a 3 times less dense foil with  $n_e/n_c = 27$  (but 3 times larger thickness to keep the

areal mass constant, as is the case when the foil would expand). Clearly, the cutoff is shifted to the 5th order, which is close to the plasma frequency  $\omega_p/\omega_0 = \sqrt{27} = 5.2$ . From this result we conclude that the cutoff observed in the experiment is an indication for a density in the foil close to the solid density.

The question by which mechanism are the harmonics emitted from the rear side remains. The PIC simulations show that energetic electron bunches (Brunel electrons [19]) are launched from the laser-irradiated surface and propagate periodically with the laser frequency  $\omega_0$  through the foil to the rear side. They may be viewed as an inharmonic source resonantly driving strong plasma oscillations of bulk electrons inside the foil at locations  $x_q$  where the local plasma frequency coincides with multiples of the laser frequency,  $\omega_p(x_q) = q\omega_0$  with  $q = 1, 2, \dots$ .

This is seen in Fig. 4 in terms of  $j_x$  (electron current along the target normal) plotted in the  $x, t$  plane. One clearly perceives the fundamental laser period, but also the different resonant layers oscillating at multiples of  $\omega_0$ . The plot corresponds to three laser oscillations near the peak of the laser pulse. At this time the foil has expanded somewhat, and the locations are indicated where  $n_e(x)/n_c = 1, 30$ , and  $80$ . In order to highlight the resonance layers more clearly, we show in the lower part of Fig. 4 the frequency spectra of  $j_x$ , obtained at these  $x$  locations by Fourier transform over the total pulse duration.

In the center of the foil, where  $n_e/n_c \approx 80$ , the frequency  $9\omega_0$  clearly dominates in the  $j_x$  spectrum, corresponding to the local plasma frequency

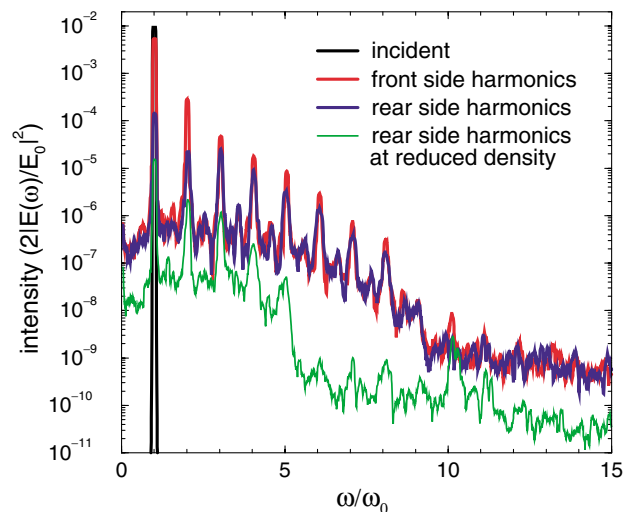


FIG. 3 (color). Simulated front (red) and rear side (blue) spectra at standard parameters (see text). Green line (for clarity it is shifted down by a factor of 10) shows the rear side spectrum at lower density  $n_e/n_c = 27$ , but the same areal mass (thickness =  $0.6\lambda$ ), while the other parameters correspond to the standard ones. To get rid of the numerical noise, the spectra were smoothed over a region of  $\Delta\omega/\omega_0 = 0.1$ .

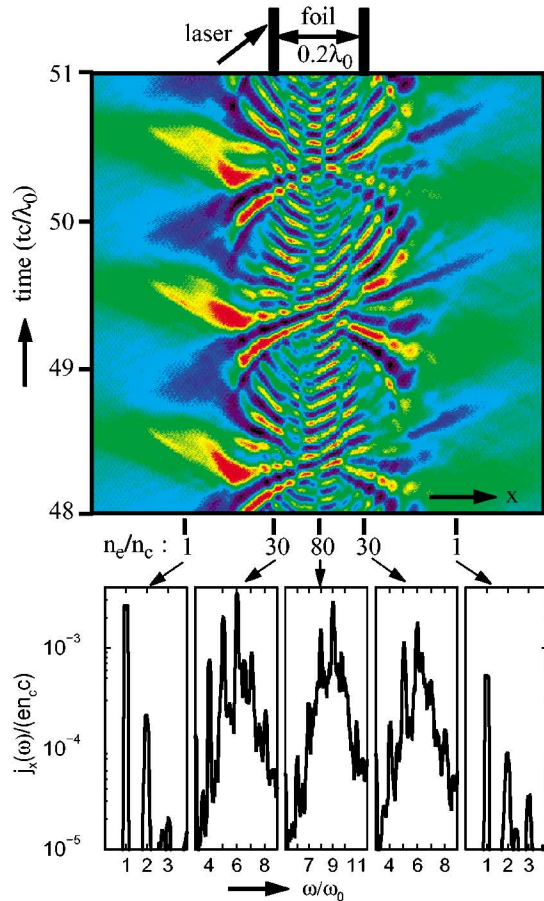


FIG. 4 (color). Current density  $j_x$  along the target normal for standard parameters. At the top, the space-time mapping of  $j_x$  (in the laboratory frame) is shown. Red corresponds to maximum positive, blue to maximum negative values, and green to zero. The thick bars indicate the unperturbed foil at  $t = 0$ . At a few positions the density at the time of the laser pulse maximum is given. The diagram at the bottom shows the Fourier spectrum of  $j_x$  at these positions, with peaks at  $\omega/\omega_0 \approx \sqrt{n_e/n_c}$ .

$\omega_p/\omega_0 = \sqrt{n_e/n_c} \approx 9$ . In the same way, the 5th and 6th harmonic dominate at  $n_e/n_c \approx 30$  and the fundamental at  $n_e/n_c \approx 1$ , respectively. Of course, the fundamental component is much stronger on the left side of the foil, where it is driven directly by the laser, but the important result of this Letter is that the fundamental and the harmonic frequencies also show up on the right side of the foil, where they are driven indirectly by the laser-generated Brunel electrons. For laser light obliquely incident in the  $x, y$  plane, also  $j_y$  currents are driven, and both  $j_x$  and  $j_y$  depend on the  $y$  coordinate by the same phase factor as the incident light vector. This implies that the currents in the right half of the foil are a source of electromagnetic radiation, which is emitted from the rear surface with same direction and polarization as the incident light. The rear side spectrum contains frequencies that are resonantly enhanced. It is cut off at the plasma frequency corresponding to the maximum density of the foil. This explains the observations.

We have also changed parameters in the simulations. We observe still rear side harmonics at reduced intensity. In the range  $1 \leq a_0 \leq 0.25$  (at otherwise standard conditions), we find for the efficiency of the 7th harmonic the scaling  $\eta_7 \propto I_L^\alpha$ , with  $\alpha \approx 1.2$ , which corresponds to the experimental finding. Increasing the foil thickness (again at otherwise standard conditions), a significant decrease of the rear side harmonic efficiency occurs at foil thicknesses above  $d_f \geq \lambda_0$ , i.e., at somewhat thicker foils than in the experiment [Fig. 2(b)]. No harmonics are generated at the rear side, when the polarization of the incident laser beam is changed from  $p$  to  $s$  or when the angle of incidence is changed from  $45^\circ$  to normal incidence ( $0^\circ$ ). In these cases no Brunel electrons are excited, and the mechanism described above does not exist.

In summary, we experimentally observed the emission of harmonics from the rear side of laser-irradiated thin foils, which remain overdense during the interaction. From PIC calculations we conclude that the harmonic emission is caused by electric currents flowing in the foil in a region where the harmonic frequency  $q\omega_0$  is close to the local plasma frequency. The excitation of these resonant currents is attributed to energetic electrons propagating from the interaction zone into the foil. The highest harmonic generated in this way is near the plasma frequency of the dense foil. Above this frequency a cutoff occurs, which is observed in the experiment and the simulation and is of interest for diagnostics to determine the maximum density in the foil during the interaction.

This work was supported in part by the European Communities in the Framework of the Euratom-IPP Association and the Deutsche Forschungsgemeinschaft (DFG Grants No. TE190/4-1 and No. TS82/1-1).

- [1] S.V. Bulanov *et al.*, Phys. Plasmas **1**, 745 (1994).
- [2] N.H. Burnett *et al.*, Appl. Phys. Lett. **31**, 172 (1977); R.L. Carman *et al.*, Phys. Rev. Lett. **46**, 29 (1981).
- [3] S. Kohlweyer *et al.*, Opt. Commun. **117**, 431 (1995).
- [4] D. von der Linde *et al.*, Phys. Rev. A **52**, R25 (1995).
- [5] P.A. Norreys *et al.*, Phys. Rev. Lett. **76**, 1832 (1996).
- [6] R. Hässner *et al.*, Opt. Lett. **22**, 1491 (1997).
- [7] M. Zepf *et al.*, Phys. Rev. E **58**, R5253 (1998); A. Tarasevitch *et al.*, Phys. Rev. A **62**, 023816 (2000).
- [8] I. Watts *et al.*, Phys. Rev. Lett. **88**, 155001 (2002).
- [9] U. Teubner *et al.*, Phys. Rev. A **67**, 013816 (2003).
- [10] R. Lichters *et al.*, Phys. Plasmas **3**, 3425 (1996).
- [11] P. Gibbon, IEEE J. Quantum Electron. **33**, 1915 (1997).
- [12] L. Plaja *et al.*, J. Opt. Soc. Am. B **15**, 1904 (1998).
- [13] W. Theobald *et al.*, Phys. Rev. Lett. **77**, 298 (1996).
- [14] P. Gibbon *et al.*, Phys. Rev. E **55**, R6352 (1997).
- [15] D. Giulietti *et al.*, Phys. Rev. Lett. **79**, 3194 (1997).
- [16] J. Fuchs *et al.*, Phys. Rev. Lett. **80**, 2326 (1998).
- [17] T. Kawachi *et al.* (to be published).
- [18] K. Eidmann *et al.*, Phys. Rev. E **62**, 1202 (2000).
- [19] F. Brunel, Phys. Rev. Lett. **59**, 52 (1987).